Mineralogy and Petrology (2002) 75: 245–259

Mineralogy and Petrology

Multiple phase transitions of leonite-type compounds: optical, calorimetric, and X-ray data

B. Hertweck[1], **T. Armbruster**[2], and **E. Libowitzky**[1]

[1] Institut für Mineralogie und Kristallographie, Universität Wien – Geozentrum, Wien, Austria
[2] Laboratorium für chemische und mineralogische Kristallographie, Universität Bern, Bern, Switzerland

With 6 Figures

Received March 7, 2001;
revised version accepted June 27, 2001

Summary

Low-temperature phase transitions of leonite-type compounds, $K_2Me^{2+}(SO_4)_2 \cdot 4H_2O$ (Me = Mg, Mn, Fe), are investigated by temperature dependent measurements of single-crystal X-ray reflection intensities and lattice parameters. The transition temperatures and the progress of the transitions are determined by birefringence data and differential scanning calorimetry. The cause for the phase transitions of leonite-type compounds is a dynamic disorder of sulphate groups at room temperature ($C2/m$), that freezes in to an ordered structure ($I2/a$) at $-4(1)\,^{\circ}C$ in leonite, $K_2Mg(SO_4)_2 \cdot 4H_2O$. At $-153(1)\,^{\circ}C$ the crystal structure switches to another ordered phase ($P2_1/a$). The Mn analogue shows the same succession with transition temperatures at $-68(1)\,^{\circ}C$ and $-104(1)\,^{\circ}C$. The disordered room temperature structure of the isotypic mineral mereiterite, $K_2Fe(SO_4)_2 \cdot 4H_2O$, transforms directly to the ordered $P2_1/a$ structure at $3(2)\,^{\circ}C$.

Analysis of X-ray intensities and of excess birefringence reveals that the displacive $I2/a \Leftrightarrow P2_1/a$ phase transition of leonite and Mn-leonite is first order. According to Landau theory the $C2/m \Leftrightarrow I2/a$ (leonite, Mn-leonite) and $C2/m \Leftrightarrow P2_1/a$ (mereiterite) order-disorder transitions are almost tricritical.

Introduction

The determination of the changes in free energy associated with structural phase transitions is an important task in the investigation of thermodynamic properties of minerals. With calorimetric methods enthalpy and entropy changes can be

independently investigated, and together with microscopic models of the atomic structure the thermodynamics of the structural changes can be calculated. Another approach is to investigate macroscopic properties such as strain (*Carpenter* et al., 1998) and optical birefringence (*Fousek* and *Petzelt*, 1979). If the mathematical form of the relationship between the excess free energy related to the phase transitions and the changes in some macroscopic properties is known, easily measurable properties can provide quantitative thermodynamic data (*Landau* and *Lifshitz*, 1980; *Tolédano* and *Tolédano*, 1987; *Carpenter*, 1992).

The minerals leonite, $K_2Mg(SO_4)_2 \cdot 4H_2O$, and mereiterite, $K_2Fe(SO_4)_2 \cdot 4H_2O$, as well as synthetic Mn-leonite, $K_2Mn(SO_4)_2 \cdot 4H_2O$, belong to a group of isotypic compounds with space group $C2/m$ at room temperature. Previous structure investigations have shown that one of the sulphate groups is disordered at room temperature (*Srikanta* et al., 1968). Refinements of single-crystal X-ray data at ambient and low temperatures (*Hertweck* et al., 2001) indicated that the dynamic disorder of leonite and Mn-leonite freezes in to an ordered structure (space group $I2/a$) at low temperatures. Upon further cooling, the ordered arrangement switches to another modification (space group $P2_1/a$) with a different sulphate-ordering scheme. Mereiterite shows only one transition from the disordered structure at room temperature to an ordered sulphate arrangement in space group $P2_1/a$ at low temperature.

In the present study, the two successive structural transitions $C2/m \Leftrightarrow I2/a \Leftrightarrow P2_1/a$ of leonite and Mn-leonite and the $C2/m \Leftrightarrow P2_1/a$ phase transition of mereiterite are compared to each other. Both low-temperature space groups ($I2/a$, $P2_1/a$) are subgroups of the $C2/m$ room temperature space group. To facilitate direct comparison between the atomic arrangement of these structures, a non standard orientation has been chosen for the two low-temperature phases. The sudden transition of the structures of leonite and Mn-leonite from one ordered low-temperature space group to the other ($I2/a \Leftrightarrow P2_1/a$) does not show a sub/supergroup relation.

Symmetry changes are pursued by investigating the intensities of several X-ray reflections as a function of temperature. Volume properties are obtained by X-ray diffraction, measuring the lattice parameters as a function of temperature. Differential scanning calorimetry (DSC) is used to measure the heat-capacity changes during the transformation processes. Changes of birefringence with decreasing temperature give a measure of the progress of the transformations. The symmetry information, as well as thermodynamic data like volume and thermal properties, and also the optic behaviour as macroscopic property are related to each other by Landau theory to reveal the thermodynamic character of the phase transitions of leonite-type compounds.

Experimental

Transparent single-crystals of $K_2Me(SO_4)_2 \cdot 4H_2O$ were obtained by controlled evaporation of an aqueous solution of an equimolar mixture of K_2SO_4 and $MeSO_4 \cdot nH_2O$ (Me = Mg, Mn, Fe). Colourless crystals of leonite were synthesised at 90 °C, pink crystals of Mn-leonite were obtained at room temperature, and brownish yellow crystals of mereiterite were synthesised at 60 °C. The compounds

crystallise tabular (100) and elongated parallel to [001], up to 2.5 cm long for leonite and up to 5 cm for Mn-leonite. The elongation is only about 0.2 cm for mereiterite, which especially tends to occur anhedrally intergrown and with lamellar twinning on {100}.

Temperature-dependent X-ray intensities of selected reflections were measured on an Enraf-Nonius CAD4 single-crystal diffractometer using graphite monochromatised MoK_α radiation. Isometric fragments of the crystals (diameter ~ 0.2 mm) of leonite, Mn-leonite and mereiterite were mounted on a silica-glass needle using a temperature-resistant epoxy resin. Data were collected using 1.5° wide ω-scans. A conventional liquid nitrogen cooling device with an accuracy of ± 2 °C was used for the collection of X-ray data between -174 °C (leonite), -158 °C (Mn-leonite), or -142 °C (mereiterite), respectively, and room temperature. The exact temperatures were calibrated after the experiment by flushing the thermocouple mounted at the crystal position with liquid nitrogen. Lattice parameters were refined from 14 reflections in the range 20–36° θ at several different temperatures within the measured interval.

Additional single-crystal X-ray data of mereiterite were collected on a Nonius Kappa CCD single-crystal diffractometer equipped with a fiber optics collimator using graphite monochromatised MoK_α radiation. Lattice parameters were determined from 50 frames measured in temperature steps of 5–10° in the range between -93 and 97 °C. In the low-temperature range an Oxford Cryostream liquid nitrogen cooling device was used.

For optical investigations crystal fragments of leonite, Mn-leonite and mereiterite, 3–4 mm in size, were oriented parallel to (100) on the basis of morphology and mounted on a self-constructed crystal grinder. They were ground with SiC abrasive paper and polished on both sides with γ-Al_2O_3 films. The final thickness t of the crystal slabs was between 400 and 600 µm.

The retardation $t \cdot (n'_\gamma - n_\alpha)$ (birefringence $\Delta n'_{\alpha\gamma} = n'_\gamma - n_\alpha$) versus temperature in the range of -195 to 100 °C was measured on a Leitz MPV2 microscope equipped with a LINKAM THMS 600 heating/cooling stage (accuracy ± 1 °C) and a Leitz monochromator (accuracy ± 1.5 nm). The orientation of the optical indicatrix was determined by *Giester* and *Rieck* (1995) on mereiterite. The crystal slabs were adjusted to show maximum interference colours under crossed polarizers (45° position), and the wavelengths of the monochromatic light, yielding maximum extinction, were determined versus temperature as a measure of retardation. Because the wavelength dispersion of the birefringence influences the results obtained by this method, $\Delta n'_{\alpha\gamma}$ was determined at three wavelengths for each compound. The crystal slabs were heated and cooled between -195 °C and 100 °C in steps of 5 °C, close to the transition points in steps of 1 °C, with a cooling rate of 10 °C per minute. The temperatures were kept constant to ± 0.2 °C. Details of this technique are described by *Libowitzky* and *Armbruster* (1995).

For differential scanning calorimetry measurements the samples were ground to powders and filled into aluminium crucibles. A Mettler Toledo 821e differential scanning calorimeter was used for the measurements with an empty aluminium crucible as reference. The samples were scanned between -120 °C and room temperature with a heating and cooling rate of 1 °C/min. The transition temperatures are defined by the onset of the DSC curves. The onset is given by the

intersection of two tangents: one applied to the baseline, the other one applied to the signal flank.

Results

The symmetry changes and the exact transition temperatures of the successive structural transitions were determined by the temperature dependent evolution of the X-ray reflection intensities of several (see Table 1) strong reflections violating the extinction rules for body centred structures (for $I2/a \Leftrightarrow P2_1/a$) and for C-centred structures (for $C2/m \Leftrightarrow I2/a$ and $C2/m \Leftrightarrow P2_1/a$). To obtain additional information about the character of the phase transitions, lattice parameters were refined from 14 reflections (Table 1) at discrete temperatures within the measured interval. The intensities of several X-ray reflections vs. temperature are plotted in Fig. 1, the variation of lattice parameters (a, b, c, β) with temperature is shown in Fig. 2.

With increasing temperature, the $h+k+l \neq 2n$ X-ray reflections of the $P2_1/a$ phases of leonite and Mn-leonite, contradicting the body-centred lattice, disappear suddenly at the $I2/a \Leftrightarrow P2_1/a$ phase transition. The observed transition temperatures are $-160(2)\,^{\circ}C$ for leonite and $-106(2)\,^{\circ}C$ for Mn-leonite, respectively. The $h+k \neq 2n$ (with $l \neq 2n$) X-ray reflections of the $I2/a$ phase, contradicting the C-centred lattice, decrease in intensity with increasing temperature and finally disappear at the $C2/m \Leftrightarrow I2/a$ phase transition, which is observed at $-8(1)\,^{\circ}C$ for leonite and $-71.5(10)\,^{\circ}C$ for Mn-leonite. Because the data points in the region of the $C2/m \Leftrightarrow I2/a$ transition temperature are not close enough, the transition temperatures are determined by a rough fit of the intensity vs. temperature curves, using a 2nd order polynomial. Generally, the transition temperatures of leonite and Mn-leonite indicated by X-ray data are 4–8 °C lower than those indicated by optical and calorimetric data (see below).

Both phase transitions hardly affect the cell volumes, which increase linearly with increasing temperature. However, the a lattice parameters generally show an anomalous temperature dependence, i.e., decreasing with increasing temperature across the measured stability range of the three phases. Especially in the stability range of the $I2/a$ and the $C2/m$ phases up to room temperature the a lattice parameters show a thermal expansion of $-11 \cdot 10^{-6}\,K^{-1}$ for leonite and $-14.5 \cdot 10^{-6}\,K^{-1}$ for Mn-leonite. At the $I2/a \Leftrightarrow P2_1/a$ phase transition of leonite and Mn-leonite the curves of the temperature dependencies of the a lattice parameters and the β angles show a discontinuity, i.e., a sudden increase of ~ 0.013 Å for a and a decrease of $\sim 0.05\,^{\circ}$ for β. The $C2/m \Leftrightarrow I2/a$ phase transition does not affect the cell dimensions within estimated standard deviations.

Skipping the intermediate $I2/a$ phase, the $h+k \neq 2n$ reflection intensities vs. temperature of the mereiterite structure at the $C2/m \Leftrightarrow P2_1/a$ phase transition appear with a similar slope as the $C2/m \Leftrightarrow I2/a$ order-disorder phase transition of the other two compounds (Fig. 1). However, discontinuities in the temperature dependence of the a and c lattice parameters of mereiterite can be observed, in contrast to the continuous evolution of the lattice parameters of leonite and Mn-leonite, which are not affected by the $C2/m \Leftrightarrow I2/a$ order-disorder phase transition (Fig. 2). The phase transition temperature of mereiterite, which is indicated by optical and calorimetric data at 3(1) °C, is confirmed by the X-ray data.

Table 1. *14 reflections in the range between 20–36° θ were used to refine the lattice parameters for leonite, Mn-leonite and mereiterite between −174 to 20°C. X-ray intensities of selected reflections were pursued in the same temperature interval*

Lattice parameter refinement						Reflection intensity measurement														
Leonite			Mereiterite			$P2_1/a \Leftrightarrow I2/a$						$I2/a \Leftrightarrow C2/m$						$P2_1/a \Leftrightarrow C2/m$		
Mn-leonite						Leonite			Mn-Leonite			Leonite			Mn-Leonite			Mereiterite		
0	0	32	12	0	0	3	−6	6		"		−3	2	3		"		0	−1	4
0	0	−32	−12	0	0	4	3	−6		"		−5	2	7		"		1	−2	4
0	16	0	0	12	0	4	−7	4		"		−1	−4	−1		"		1	−2	3
0	−16	0	0	−12	0	4	1	−4		"		−3	−8	−1		"		2	3	−3
18	0	0	0	0	12	5	2	−6		"		−1	2	7		"		3	−6	3
−18	0	0	0	0	−12	0	−3	8		"					3	1	−2	4	3	−4
12	8	16	8	8	6	4	3	−8	7	2	−6				7	1	6	4	−7	2
−12	−8	−16	−8	−8	−6	5	−6	4	8	−3	4							5	2	−3
12	8	−16	−8	8	6				0	−1	8							5	−6	2
−12	8	16	8	−8	6													5	−4	0
12	−8	16	8	8	−6													4	−9	0
−12	−8	16	−8	−8	6															
12	−8	−16	8	−8	−6															
−12	8	−16	−8	8	−6															

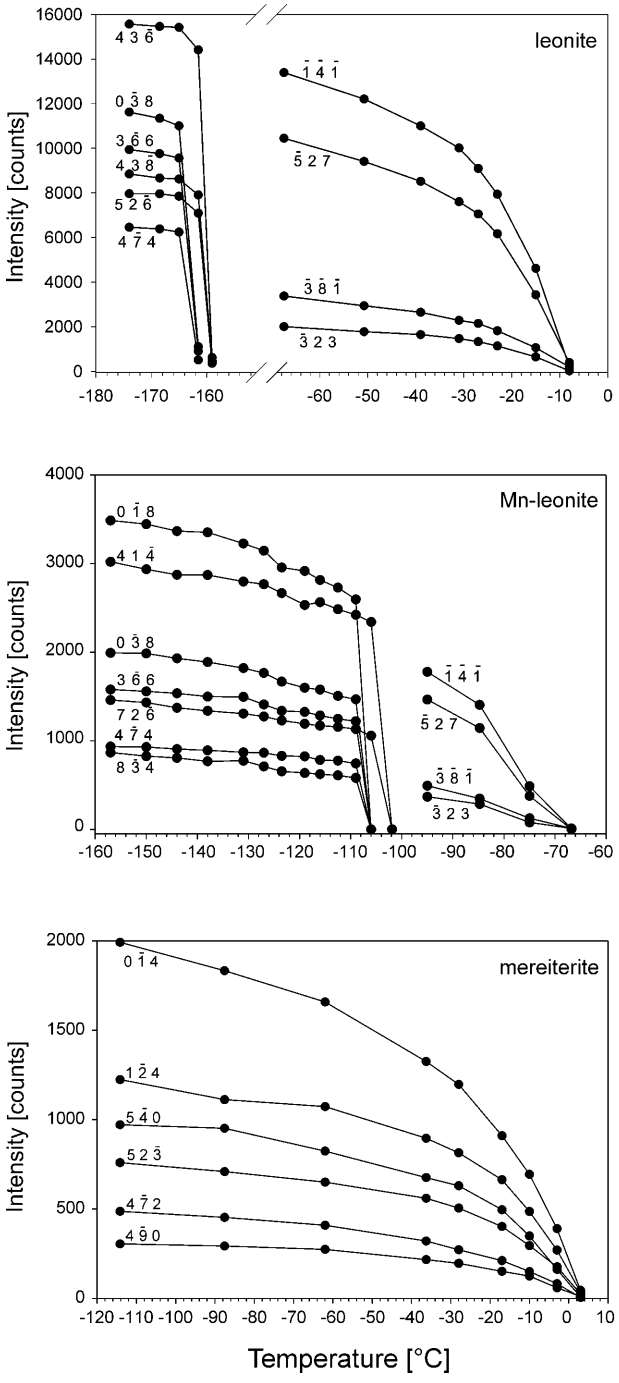

Fig. 1. Intensity versus temperature plot of distinct X-ray reflections of leonite, Mn-leonite, and mereiterite. Errors in temperature and intensity are within the size of the plotted data points

In general, at the transition to the $P2_1/a$ structures the three compounds show a discontinuity, resulting in smaller a lattice parameters (Fig. 2). However, as indicated by two independent X-ray diffraction measurements, the a lattice parameter in the $P2_1/a$ phase of mereiterite shows a further decrease, reaching the

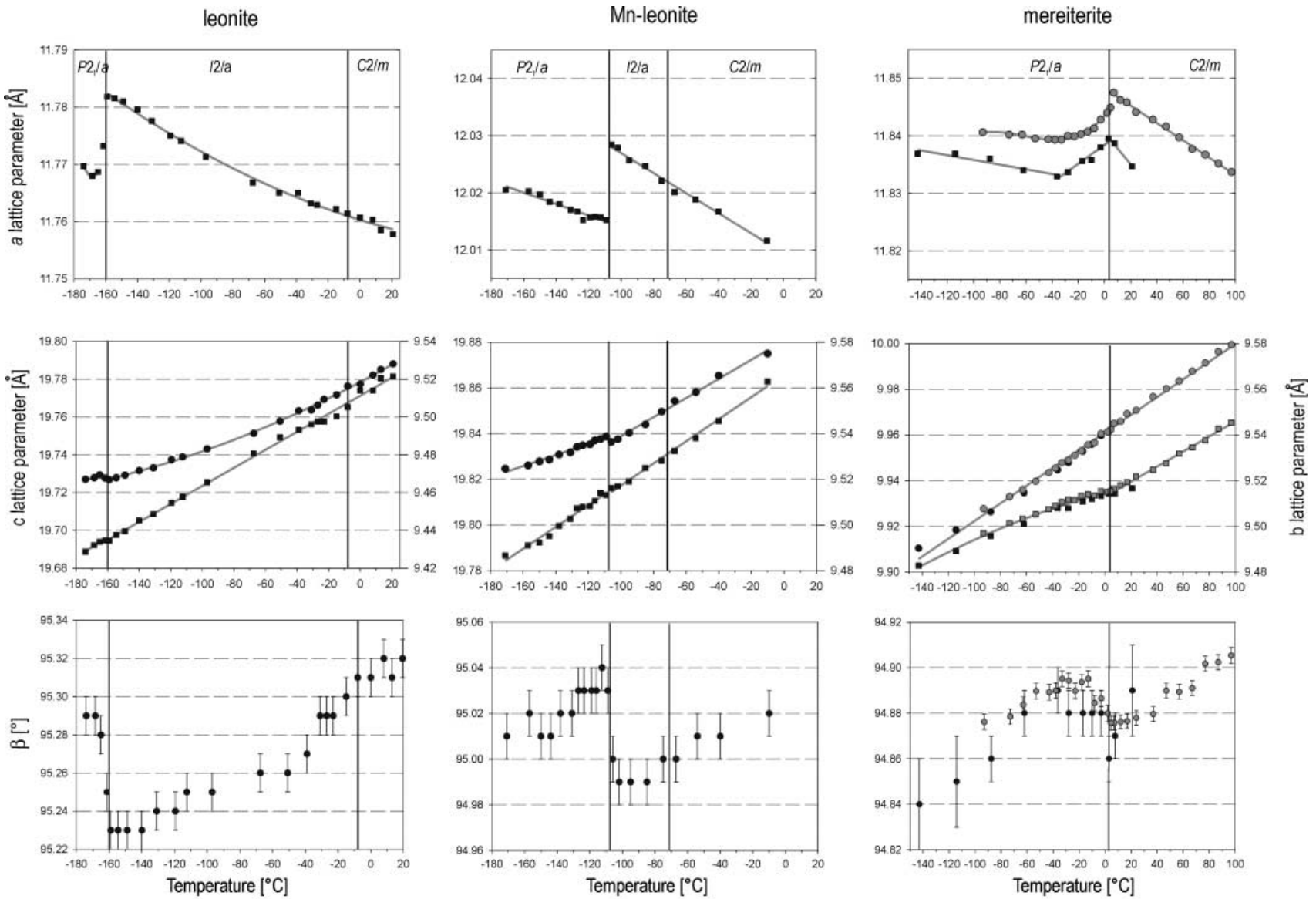

Fig. 2. Lattice parameters of leonite, Mn-leonite, and mereiterite versus temperature. The vertical lines represent the transition temperatures. The *b* lattice parameters are presented as circles, the *c* lattice parameters as squares. Data collection of the lattice parameters of mereiterite was done on one crystal on a CAD4 single-crystal diffractometer (black data points) and on a CCD diffractometer (grey data points). Errors in temperature and lattice parameters *a*, *b*, *c* are within the size of the plotted data points. Error bars are plotted for the β angles

minimum $\sim 20\,^{\circ}$ below the transition temperature. By this protracted decrease, the discontinuity at the $C2/m \Leftrightarrow P2_1/a$ transition of mereiterite appears smaller than the $I2/a \Leftrightarrow P2_1/a$ transition of leonite and Mn-leonite.

The optical and calorimetric data confirm the two reversible phase transitions for leonite and Mn-leonite and the single transition of mereiterite. A plot of the birefringence data ($\Delta n'_{\alpha\gamma} = n'_{\gamma} - n_{\alpha}$) vs. temperature in the range between $-195\,^{\circ}$C to $100\,^{\circ}$C is given in Fig. 3. Each plotted birefringence curve is the average of three measurements at different wavelengths. The wavelength dispersion of this experimental technique, however, may cause slight inaccuracies, that interfere with the precise determination of the excess birefringence (*Libowitzky* and *Armbruster*, 1995).

The birefringence values of leonite increase linearly with decreasing temperature towards the $C2/m \Leftrightarrow I2/a$ phase transition point at $-4\,^{\circ}$C. At the transition point the slope increases discontinuously. Upon further cooling the birefringence values increase non-linearly towards the $I2/a \Leftrightarrow P2_1/a$ phase transition point at $-152.5\,^{\circ}$C, which is indicated by a discontinuity, i.e., a jump of the birefringence value by 0.0001. Below the second phase transition point the birefringence continues to increase linearly. The slope of the birefringence values for Mn-leonite is similar to that of leonite, with phase transition temperatures indicated at $-68\,^{\circ}$C and $-103.5\,^{\circ}$C. The nonlinear increase of the birefringence values of mereiterite indicates one phase transition at $2\,^{\circ}$C.

Determination of the excess birefringence of the phase transitions required baselines, which were obtained by fits of a 2nd order polynomial to the

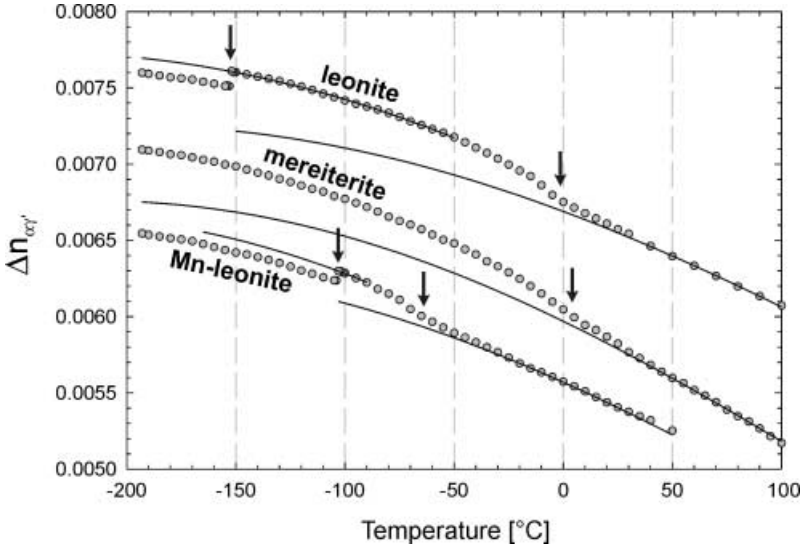

Fig. 3. Temperature dependence of the optical birefringence $\Delta n'_{\alpha\gamma}$ of leonite, Mn-leonite and mereiterite. The transition temperatures are indicated by arrows. Baselines (solid lines) to determine the excess birefringences are fitted using a rational equation for the order-disorder phase transitions and a 2nd order polynomial for the second phase transition of leonite and Mn-leonite

experimental data in the range of the $I2/a \Leftrightarrow P2_1/a$ phase transition and by fits of the rational equation $y = (a + b * x)/(1 + c * x + d * x^2)$ to the experimental data in the range of the $C2/m \Leftrightarrow I2/a$ ($P2_1/a$ in mereiterite) phase transition. The rational equation was chosen, because it describes best the shape of the birefringence curves with a linear flank turning into a curvature. Taking into account pre-transitional effects at the order-disorder phase transition, indicated by a deviation

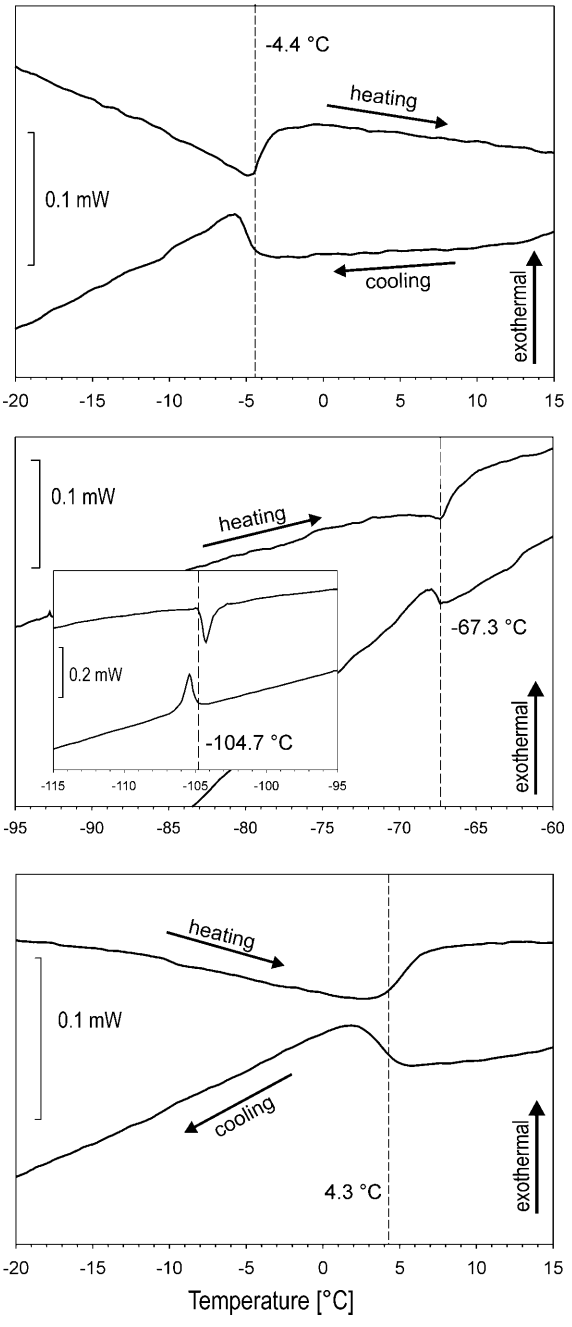

Fig. 4. DSC measurements of leonite (upper), Mn-leonite (middle) and mereiterite (lower) with 1 °C/min heating and cooling rate. Normalised on 10 mg. Large plots show the order-disorder phase transitions $C2/m \Leftrightarrow I2/a$ ($P2_1/a$). The inset shows the $I2/a \Leftrightarrow P2_1/a$ phase transition in Mn-leonite. Dashed lines indicate transition temperatures

from the linear behaviour above T_c, only data points $\sim 40\,^\circ$ above the phase transition temperature were used. Similar and more pronounced pre-transitional effects were observed, e.g., in lawsonite (*Sondergeld* et al., 2000).

Three graphs showing the differential scanning calorimetry (DSC) measurements are given in Fig. 4. Since the temperature range of the DSC is $-150\,^\circ$C to $600\,^\circ$C, it was not possible to measure the temperature of the second phase transition point of leonite, which is indicated by optical and X-ray data to be in the range of $-152\,^\circ$C to $-160\,^\circ$C. In the graphic presentations of the DSC measurements the areas enclosed by a baseline and by the DSC curves correspond to the transition heat.

The DSC measurements indicate transition temperatures for the first phase transition at $-4.4\,^\circ$C for leonite, $-67.3\,^\circ$C for Mn-leonite (both $C2/m \Leftrightarrow I2/a$), and $4.3\,^\circ$C for mereiterite ($C2/m \Leftrightarrow P2_1/a$). The peaks are broad and weak (peak maximum ~ 0.02 mW) with a hysteresis range of $\sim 1\,^\circ$C. Below the phase transition temperatures the change of the heat capacity of the samples is correlated with a change of the slope of the baseline. Upon further cooling the second phase transition ($I2/a \Leftrightarrow P2_1/a$) is indicated by a narrow, sharp, and strong (~ 0.12 mW) peak at $-104.7\,^\circ$C for Mn-leonite. Below the second phase transition temperature the slope of the baseline is maintained.

Discussion

Structural phase transitions can be classified by the characteristics of thermodynamic quantities such as volume (see cell dimensions in Fig. 2) and thermal properties (see calorimetric data in Fig. 4). For the calculation of the Gibbs free energy, however, all entropy contributions had to be separately assessed. Hence, calculations of the thermodynamics of structural changes had to involve structural models to attempt to describe the variations in free energy from interaction energy between atoms.

A different approach to determine free energy changes is to measure changes in macroscopic properties such as strain or optical birefringence (Fig. 3), that are related to atomic interactions. For the phase transitions of leonite-type compounds the structural mechanism involved has already been revealed by single-crystal structure analysis (*Hertweck* et al., 2001) and can be related to the thermodynamic classification. The distortion of the structure, mainly due to the rotation of the sulphate groups in the leonite-type compounds, leads to a change in shape of the unit cell and to a distortion of the optical indicatrix. This is expressed in terms of spontaneous strain and a change of birefringence (Fig. 3). In addition, the change of symmetry through the phase transitions is expressed by the evolution of X-ray intensities (Fig. 1) as a function of temperature.

The relationship between the changes in free energy and the changes in some macroscopic properties is defined mathematically by Landau theory (*Landau* and *Lifshitz*, 1980; *Tolédano* and *Tolédano*, 1987; *Carpenter*, 1992). The evolution of the order parameter Q with temperature, central concept of Landau theory, describes the thermodynamic character of a phase transition. The correct form of the order parameter and its relationship to certain measurable physical

properties for a given change in symmetry is listed in standard tables (e.g., *Carpenter*, 1992).

The excess free energy ΔG due to a phase transition can be described as a polynomial expansion of the order parameter Q, with coefficients α, A, b, B, etc., which may depend on material properties and/or on extensive variables such as temperature or pressure. Although this calculation concerns the *excess* free energy ΔG, the notation G is used in further discussion for simplification. To satisfy the equilibrium criteria above T_c, the free energy expansion becomes

$$G = a/2(T - T_c)Q^2 + b/3\ Q^3 + B/4\ Q^4 + \cdots .$$

The form of the free energy expansion is determined by the nature of the phase transition (*Carpenter*, 1992). Hence, certain aspects of the leonite-type crystal structures are elucidated to correlate the free energy calculations from experimental birefringence, calorimetric and X-ray data with the structural transition behaviour.

At room temperature the leonite-type compounds crystallise in space group $C2/m$. Refinements of single-crystal X-ray diffraction data indicate a dynamic disorder of sulphate tetrahedra (*Srikanta* et al., 1968). Units of MeO_6 octahedra with two sulphate tetrahedra in *trans* conformation are connected by hydrogen bonds, forming layers parallel to (001). A schematic plot of the structure is given in Fig. 5. According to this formal description (*Hertweck* et al., 2001) layers of octahedra and ordered tetrahedra alternate with layers of octahedra and disordered tetrahedra along [001] in the form of an AB stacking. The orientation of the dynamically disordered tetrahedra, pointing along [010] or $[0\bar{1}0]$ in time and space average, alternates along [100] within the layer. A mirror plane parallel to (010) intersects the layers of octahedra and tetrahedra.

Below the transition temperature the dynamic disorder of the sulphate tetrahedra freezes in (*Hertweck* et al., 2001) to an ordered structure of leonite and Mn-leonite in space group $I2/a$ (Fig. 5). The [010] or $[0\bar{1}0]$ pointing tetrahedra within the formerly disordered layers show a reverse order in the next corresponding layer. Due to this AB′AB″ stacking along [001] the c lattice parameter is doubled and the structure is described in a body-centred monoclinic lattice. Mereiterite transforms from the $C2/m$ room temperature phase to a low-temperature $P2_1/a$ phase by loss of both the mirror plane and the two-fold axis (Fig. 5), i.e., for mereiterite the transition consists only of one symmetry reduction without changing the unit cell shape (structure description see below). Both low-temperature space groups $I2/a$ (leonite, Mn-leonite) and $P2_1/a$ (mereiterite) are subgroups of the $C2/m$ room temperature space group by symmetry reduction.

These $C2/m \Leftrightarrow I2/a$ (leonite, Mn-leonite) and $C2/m \Leftrightarrow P2_1/a$ (mereiterite) order-disorder transitions proceed continuously, as indicated by the kind of change of the birefringence (Fig. 3), by the kind of the DSC signal (Fig. 4) or by the continuous disappearance of the symmetry-forbidden X-ray intensities (Fig. 1). The strongest evidence for a continuous transition are the changing unit cell dimensions as a function of temperature nearly without excess change, at least in leonite and Mn-leonite (Fig. 2).

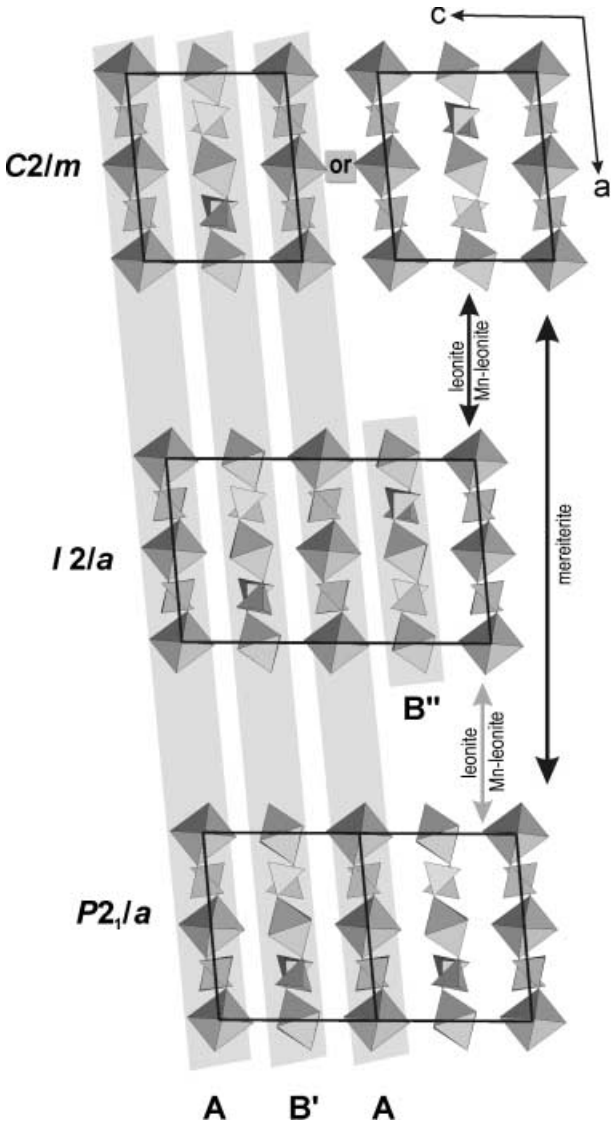

Fig. 5. Schematic picture of the crystal structures of the leonite-type compounds. The arrows show the reversible phase transitions between the room temperature phase (space group $C2/m$) and the low-temperature phases (space groups $I2/a$ and $P2_1/a$). The crystal structures are plotted without potassium ions and water molecules. Black arrows show supergroup/subgroup relationships between the room temperature structure and both low-temperature derivatives. Groups of octahedra with two tetrahedra form layers parallel to (001). The layers with the ordered tetrahedra are indicated as A, the layers with the disordered tetrahedra are indicated as B

Two terms of the free energy expansion are sufficient to describe the free energy changes of the $C2/m \Leftrightarrow I2/a$ (leonite, Mn-leonite) and $C2/m \Leftrightarrow P2_1/a$ (mereiterite) order-disorder transitions using the experimentally measured intensities of certain X-ray reflections (*Carpenter*, 1992) and the excess birefringence

(*Fousek* and *Petzelt*, 1979; *Fuith* and *Kroupa*, 1990), which both correspond to the squared order parameter Q. The free energy expansion appears in the form:

$$G = a/2(T - T_c)Q^2 + c/6\ Q^6$$

Odd-order coefficients are absent in the expansion and with $c > 0$ the transition is tricritical. By minimising G with respect to Q the equilibrium behaviour Q through the phase transition is determined:

$$Q = a/c(T_c - T)^{1/4}$$

The variation of Q with temperature is continuous between $Q = 1$ and $Q = 0$, as shown in Fig. 6a–b for leonite, Mn-leonite, and mereiterite. The critical exponent is $1/4$ for an ideal tricritical transition (*Carpenter*, 1992). Fitting of the experimental

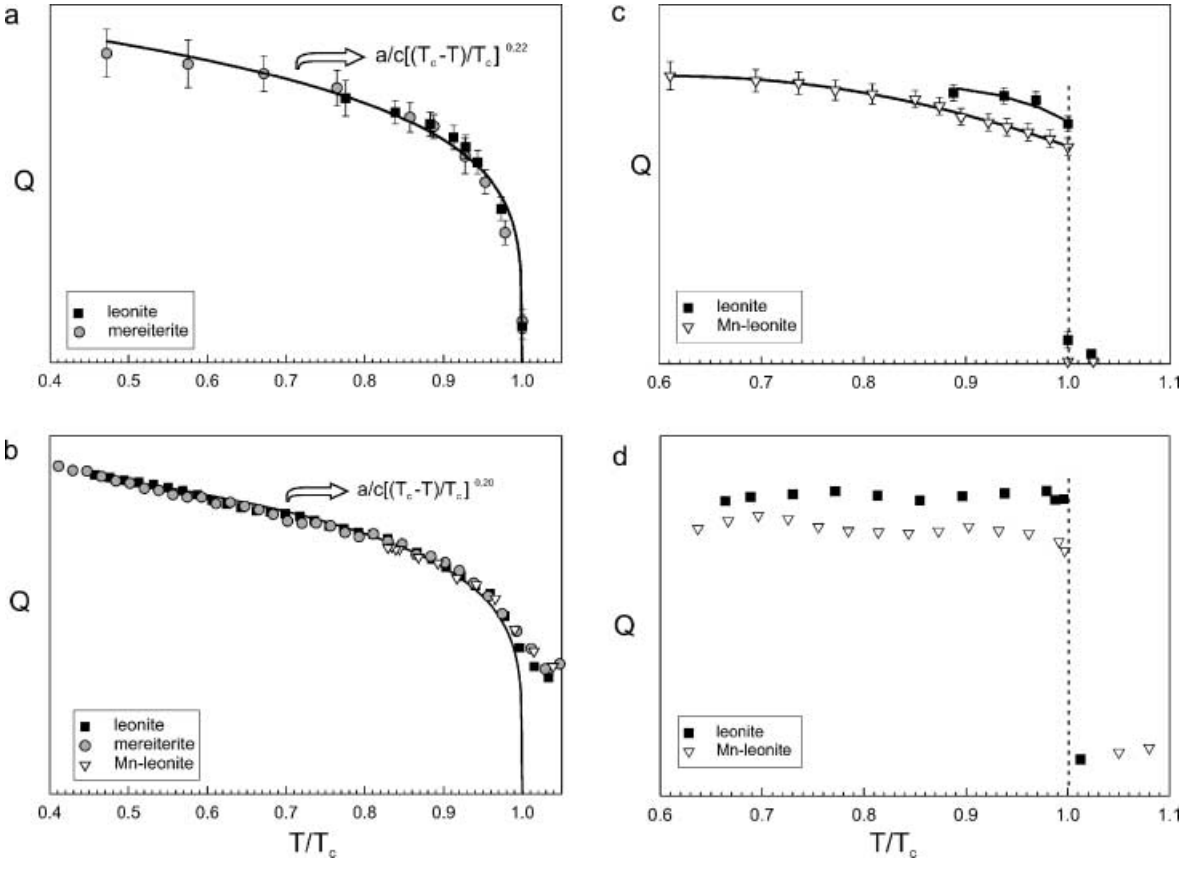

Fig. 6. Variation of the order parameter Q with temperature. Data points represent square roots of normalised X-ray reflection intensities and of normalised excess birefringence, respectively, as a function of temperature. **a** X-ray reflection intensities and **b** excess birefringence of the order-disorder phase transitions $C2/m \Leftrightarrow I2/a$ ($P2_1/a$) in leonite, Mn-leonite and mereiterite. **c** X-ray reflection intensities and **d** excess birefringence of the $I2/a \Leftrightarrow P2_1/a$ phase transition in leonite and Mn-leonite. Errors in the order parameters calculated from excess birefringences are within the size of the plotted data points

data of the X-ray intensity (Fig. 6a) and birefringence measurements (Fig. 6b) results in a critical exponent of 0.20–0.22, which is almost tricritical.

Upon further cooling the formerly disordered tetrahedra in the leonite and Mn-leonite structure change once again to another ordered arrangement, i.e., the sudden transition of the $I2/a$ crystal structure to another monoclinic phase with space group $P2_1/a$ (*Hertweck* et al., 2001). This is the space group into which mereiterite orders directly, cooling down from the disordered room temperature phase. The ordered sequence of [010] and $[0\bar{1}0]$ pointing tetrahedra within the layer and along [001] results in the loss of the two-fold axis. Thus, the layers return to the original AB stacking, comparable with the room temperature structure, but with ordered tetrahedra in both layers (*Hertweck* et al., 2001). The unit cell corresponds to the room-temperature cell size, but becomes primitive.

These displacive $I2/a \Leftrightarrow P2_1/a$ phase transitions of leonite and Mn-leonite show a discontinuity of the a lattice parameter and the β angle at the equilibrium temperature T_c (Fig. 2). This is explained by the stronger tilt of the tetrahedron-octahedron-tetrahedron groups relative to the a axis in the $P2_1/a$ structure in comparison to the $I2/a$ structure. Units of corner-sharing octahedra and SO_4 tetrahedra are developed only parallel to [100], whereas considerably weaker bonds exist between these units along [010] and [001]. Hence, a change of the structure affects the a lattice parameter and the β angle more than the b and c lattice parameter.

In addition, the discontinuity of the displacive $I2/a \Leftrightarrow P2_1/a$ phase transition is indicated by the sharp signal in the DCS measurement (Fig. 4) and by the significant discontinuity of birefringence (Fig. 3) for both leonite and Mn-leonite. The discontinuous change of the symmetry forbidden X-ray intensities is plotted in Fig. 1, where the intensities of all measured reflections disappear suddenly within a temperature interval of 2 °C, while the intensities characteristic for the $C2/m \Leftrightarrow I2/a$ or $C2/m \Leftrightarrow P2_1/a$ transitions diminish slowly over a temperature range of 20 to 40 °C.

The evolution of the X-ray reflection intensities belonging to the class $h + k + l \neq 2n$ and the progress of the excess birefringence of the $P2_1/a$ phases with increasing temperature are drawn as graphs of the order parameter Q in Fig. 6c–d. The intensity of symmetry forbidden X-ray reflections (*Carpenter*, 1992) and the excess birefringence (*Fousek* and *Petzelt*, 1979; *Fuith* and *Kroupa*, 1990), respectively, are proportional to the square of the Landau order parameter Q. A free energy expansion with a negative B coefficient correlates with the experimental data. To obtain a free energy minimum in the low-temperature phase when $Q > 0$, both a and c must be positive and the sixth-order term is required:

$$G = a/2(T - T_c)Q^2 + B/4\ Q^4 + c/6\ Q^6$$

By minimising G with respect to Q the equilibrium behaviour through the phase transition is determined. Two solutions are possible:

$$Q_{T<T_c} = \sqrt{\frac{-B + [B^2 - 4ac(T - T_c)]^{1/2}}{2c}} = Q_0 \quad Q_{T>T_c} = 0$$

This expression of the temperature evolution of the order parameter, and with that the excess free energy, describes a discontinuity at the transition temperature. This

discontinuity in Q from $Q = 0$ to $Q = Q_0$ indicates a first order phase transition for $I2/a \Leftrightarrow P2_1/a$, which is in agreement with the cell volume discontinuity at the transition temperature (Fig. 2).

Acknowledgements

B. Hertweck and *E. Libowitzky* are indebted to the Austrian Science Foundation, project P13728–GEO, who granted financial support. *G. Giester* performed the lattice parameter determination for mereiterite on the CCD diffractometer. The authors appreciate the comments of *W. Schranz* and two anonymous referees, who helped to improve the quality of the manuscript.

References

Carpenter MA (1992) Thermodynamics of phase transitions in minerals: a macroscopic approach. In: *Price GD*, *Ross NL* (eds) Stability of minerals. Chapman & Hall, London, 368 pp

Carpenter MA, *Salje EHK*, *Graeme-Barber A* (1998) Spontaneous strain as a determination of thermodynamic properties for phase transitions in minerals. Eur J Mineral 10: 621–691

Fousek J, *Petzelt J* (1979) Changes of refractive indices of crystals induced by structural phase transitions. Phys Stat Sol (a) 55: 11–40

Fuith A, *Kroupa J* (1990) Birefringence study of the 415 K phase transition in KSCN. J Phys, Condens Matter 2, 10: 2355–2359

Giester G, *Rieck B* (1995) Mereiterite, $K_2Fe(SO_4)_2 \cdot 4H_2O$, a new leonite-type mineral from Lavrion Mining District, Greece. Eur J Mineral 7: 559–566

Hertweck B, *Giester G*, *Libowitzky E* (2001) The crystal structures of the low-temperature phases of leonite-type compounds, $K_2Me(SO_4)_2 \cdot 4H_2O$ (Me = Mg, Mn, Fe). Am Mineral 86: 1282–1292

Landau LD, *Lifshitz EM* (1980) Statistical physics, 3rd edn. Pergamon Press, Oxford, 484 pp

Libowitzky E, *Armbruster T* (1995) Low-temperature phase transitions and the role of hydrogen bonds in lawsonite. Am Mineral 80: 1277–1285

Sondergeld P, *Schranz W*, *Kityk AV*, *Carpenter MA*, *Libowitzky E* (2000) Ordering behaviour of the mineral lawsonite. Phase Trans 71: 189–203

Srikanta S, *Sequeira A*, *Chidambaram R* (1968) Neutron diffraction study of the space group and structure of manganese-leonite, $K_2Mn(SO_4)_2 \cdot 4H_2O$. Acta Crystall B24: 1176–1182

Tolédano J-C, *Tolédano P* (1987) The Landau theory of phase transitions. World Scientific, Singapore, 451 pp

Authors' addresses: *B. Hertweck* and *E. Libowitzky*, Institut für Mineralogie und Kristallographie, Universität Wien – Geozentrum, Althanstraße 14, A-1090 Wien, Austria, e-mail: birgit.hertweck@univie.ac.at, eugen.libowitzky@univie.ac.at; *T. Armbruster*, Laboratorium für chemische und mineralogische Kristallographie, Universität Bern, Freiestrasse 3, CH-3012 Bern, Switzerland, e-mail: armbruster@krist.unibe.ch